Special Issue

Institution of MECHANICAL ENGINEERS

Journal of AUTOMOBILE ENGINEERING

Proc IMechE Part D: J Automobile Engineering
1–16

DOI: 10.1177/0954407016687453
journals.sagepub.com/home/pid
SAGE

An overview of the effects of fuel molecular structure on the combustion and emissions characteristics of compression ignition engines

Paul Hellier, Midhat Talibi, Aaron Eveleigh and Nicos Ladommatos

Abstract

Future fuels for compression ignition engines will be required both to reduce the anthropogenic carbon dioxide emissions from fossil sources and to contribute to the reductions in the exhaust levels of pollutants, such as nitrogen oxides and particulate matter. Via various processes of biological, chemical and physical conversion, feedstocks such as lignocellulosic biomass and photosynthetic micro-organisms will yield a wide variety of potential fuel molecules. Furthermore, modification of the production processes may allow the targeted manufacture of fuels of specific molecular structure. This paper therefore presents an overview of the effects of fuel molecular structure on the combustion and emissions characteristics of compression ignition engines, highlighting in particular the submolecular features common to a variety of potential fuels. An increase in the straight-chain length of the alkyl moiety reduces the duration of ignition delay, and the introduction of double bonds or branching to an alkyl moiety both increase ignition delay. The movement of a double bond towards the centre of an alkyl chain, or the addition of oxygen to a molecule, can both increase and decrease the duration of ignition delay dependent on the overall fuel structure. Nitrogen oxide emissions are primarily influenced by the duration of fuel ignition delay, but in the case of hydrogen and methane pilot-ignited premixed combustion arise only at flame temperatures sufficiently high for thermal production. An increase in aromatic ring number and physical properties such as the fuel boiling point increase particulate matter emissions at constant combustion phasing.

Keywords

Diesel engines, compression ignition engines, fuel design, future fuels, molecular structure, diesel engine emissions

Date received: 30 April 2016; accepted: 9 December 2016

Introduction

International recognition as to the devastating impacts of anthropogenic emissions of greenhouse gases (GHGs) on global climate change[1] has led to the requirement that future use of internal-combustion (IC) engines should result in reduced emissions of carbon dioxide (CO_2) from fossil sources relative to current levels. Concurrent to this has been the introduction of increasingly stringent legislation[2] regulating levels of toxic pollutants, such as nitrogen oxides (NO_x) and particulate matter (PM) from road transport; however, a relatively unexplored opportunity for the potentially simultaneous control of various harmful pollutants (GHGs, NO_x and PM)[3] from IC engines is by the molecular design of future fuels.

Over the course of the past 100 years in which IC engines have been in widespread use, many improvements have been made to the mechanical design and combustion strategies utilised, resulting in significantly higher engine thermal efficiencies (and thus reduced specific emissions of CO_2).[4,5] Simultaneously, exhaust after-treatment devices are now employed in both spark ignition engines and compression ignition engines

Department of Mechanical Engineering, University College London, London, UK

Corresponding author:
Paul Hellier, Department of Mechanical Engineering, University College London, Roberts Building, Torrington Place, London WC1E 7JE, UK.
Email: p.hellier@ucl.ac.uk

to ensure compliance with emissions regulations and to reduce the exhaust levels of carbon monoxide, unburned hydrocarbons, NO_x and PM. However, the use of such devices can result in increased fuel consumption and reduced engine thermal efficiency as they require a sufficiently high exhaust temperature for proper operation.[4,6]

The composition of fuels for IC engines has, however, remained relatively unchanged (with the exceptions of the removal of sulphur and the varying use of additives) and continues to be specified by the physical properties, e.g. the boiling-point range, and combustion regime specific measures such as cetane number in the case of fuels for compression ignition.[7,8] The most significant impact in recent years on the composition of fuels for IC engines within EU member states has been the regulatory requirement that biofuels must comprise a mandatory 10% minimum of gasoline and diesel consumption for road transport by 2020, as stipulated by the 2009 European Parliament Directive on the use of energy from renewable sources.[9] In the case of fuels for compression ignition engines, it has been recognised that biodiesel, which is the most commonly utilised renewable fuel component, exhibits combustion and emissions characteristics different from those of conventional fossil diesels.[10–16] However, attempts to design a fuel composition for improved engine efficiency or reduction of exhaust pollutants have not been widely reported, despite the opportunities to do so presented by the legislative need to develop renewable fuels from non-food sources.

Current liquid fuels from fossil sources are typically mixtures of straight-chain and branched-chain (iso)alkanes and (iso)alkenes, cyclic and aromatic molecules. Table 1 shows the molecular structures of typical hydrocarbon molecules contained within fossil diesel and also those of potential alternative fuel molecules from renewable sources. Although much focus has been placed on the identification of non-edible feedstocks for the production of biodiesel,[17] a wide range of chemical and biological processes are currently under study with potential for the production of fuel molecules suitable for compression ignition combustion. Alkanes, alkenes, alcohols, methane and hydrogen can be produced from genetically modified micro-organisms including photosynthetic micro-algae,[18–21] whereas catalytic upgrading of fermentation products can result in higher-weight alcohols and ketones.[22,23] Many methods of combined thermal, chemical and biological treatment of lignocellulosic biomass can produce ketones, short-chain fatty acid esters, acids, furans, methane and phenols.[24–30]

With the development of various controlled processes for the conversion of renewable energy sources to liquid fuels for compression ignition engines, in contrast with current fossil diesel, at the point of production these future fuels will likely consist of a relatively small and discrete range of species, thereby enhancing the importance of the molecular structures of the compounds present to the overall fuel characteristics. This paper therefore presents a concise review of the effects of the molecular structures of fuels on the combustion characteristics and the exhaust emissions of NO_x and

Table 1. Molecular structures of typical current and future fuels for compression ignition engines.

Alkanes and alkenes	
n-heptane	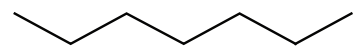
n-octane	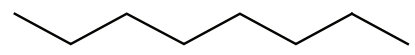
n-dodecane	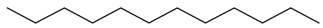
8-methylhexadecane	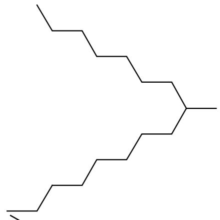
1-octene	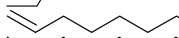
trans-3-octene	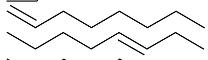
cis-3-octene	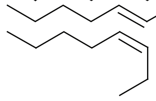
Aromatics	
Toluene	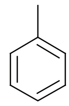
Oxygenates	
5-nonanone	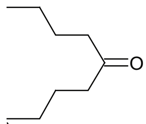
Butyl valerate	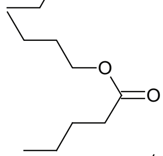
Di-*n*-butyl carbonate	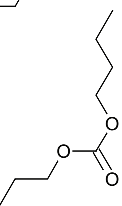
Geraniol	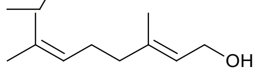
Oleic acid	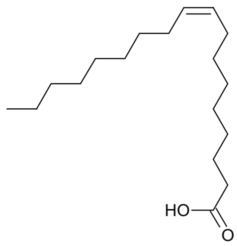
Dibutyl maleate	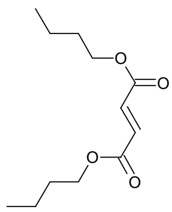
Tri(propylene glycol) methyl ester	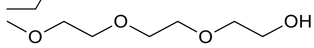

PM in modern direct-injection compression ignition engines, focusing in particular on the influence of the alkyl chains which are common to many potential fuel molecules.

Effects of the molecular structure of fuels on the duration of ignition delay

Alkyl chain length and branching

Many of the hydrocarbon and oxygenate molecules which constitute fossil fuels, current biofuels and future non-fossil alternatives (Table 1), contain at least one alkyl chain which will typically account for the majority of the molecular mass. Figure 1 shows the impact of increasing the *n*-alkane alkyl chain length on the duration of ignition delay, defined as the interval between the start of fuel injection (SOI) and the start of combustion (SOC), when tested as single-component fuels at a constant engine speed of 1200 r/min, a fuel injection pressure of 450 bar and a constant engine work output (indicated mean effective pressure (IMEP)) of 4 bar [31] The fuels were tested at two injection timings: first, constant injection at which the SOI was held constant and the SOC was allowed to vary in accordance with the ignition delay of the fuel; second, constant ignition at which the SOC was fixed at top dead centre and the SOI was varied with the duration of the fuel ignition delay. Figure 1 shows that, as the *n*-alkane alkyl chain length is increased, there is a consistent decrease in the duration of ignition delay at both injection timings. It can also be seen in Figure 1 that the addition of carbon atoms to the alkyl chain is more significant in the case of shorter-chain *n*-alkanes. For example, the addition of four carbon atoms to increase the alkyl chain length from eight atoms to 12 atoms (*n*-octane to *n*-dodecane) decreases the ignition delay by approximately 1° crank angle (CA), whereas the addition of four carbon atoms to increase the alkyl chain length from 16 atoms to 20 atoms (*n*-hexadecane to *n*-eicosane) decreases the ignition delay by about 0.5° CA. The observed diminishing decrease in ignition delay with increasing alkyl chain length concurs with measurements of the cetane numbers of *n*-alkanes,[32] and also kinetic modelling simulations of shock tube ignition delay times of C_8 to C_{16} *n*-alkanes in conditions relevant to compression ignition engines.[33] The results of these experimental investigations and modelling simulations are in agreement with the effect of alkyl chain length on rates of low-temperature radical branching reactions during the ignition delay period.[34] The progress of such reactions determines the rate at which radical species (primarily H_2O_2) accumulate and local temperatures escalate towards those required for the rapid decomposition of radicals and subsequent fuel autoignition.

Figure 2 shows the low-temperature reaction steps of hydrogen abstraction, oxygen addition and fuel molecule isomerisation required for the propagation of radical species from *n*-octane and 2-methylpentane. Rates of hydrogen abstraction increase with increasing alkyl chain length, as this results in the availability of more secondary carbon atoms (carbon atoms 2 to 7 in Figure 2(a)) which possess a lower carbon to hydrogen bond strength than primary carbon atoms (carbon atoms 1 and 8 in Figure 2(a)).[34] An increase in the alkyl chain length also increases the rates of isomerisation following oxygen addition as a greater number of sites at which six-member or seven-member transition rings are able to form become available, as this requires chains of at least three fully saturated carbon atoms.[35]

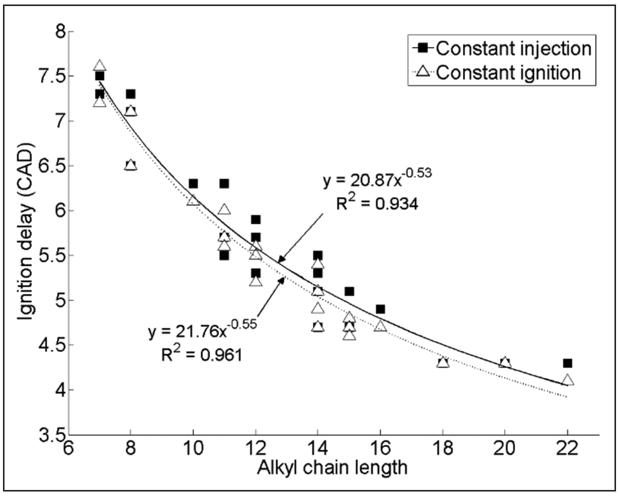

Figure 1. Effect of increasing *n*-alkane alkyl chain length on the ignition delay at constant fuel injection timing and constant SOC timing.Source: reproduced with permission from SAE International, 2011.[31]
CAD: degrees crank angle.

A decrease in ignition delay with increasing alkyl chain length has also been observed in molecules other than *n*-alkanes.[32,36,37] For example, Schönborn et al.[36] and Koivisto et al.[37] found a linear decrease in the duration of ignition delay with increasing alkyl chain length in the case of fully saturated fatty acid methyl esters (FAMEs) with alkyl chain lengths of between 12 carbon atoms to 22 carbon atoms, and primary and secondary alcohols with an alkyl chain length of between 8 carbon atoms to 16 carbon atoms, respectively. However, it is interesting to note that, in the case of fatty acid esters produced from alcohols other than methanol (and thus possessing an additional alkyl chain within the alcohol moiety of the ester), the influence of the alkyl chain length of the alcohol moiety on the duration of ignition delay is insignificant relative to that of a change in the alkyl chain length of the fatty acid moiety.[36,38–41]

The presence of alkyl chain methyl branches in *n*-alkanes[31,31] (and also in the alkyl chains of other molecules such as ethers[42] and carbonate esters[43]) has been observed to result in an increase in the duration of ignition delay. In engine tests of 8-methylhexadecane and 2,6,10,16-tetramethylpentadecane, the increase in

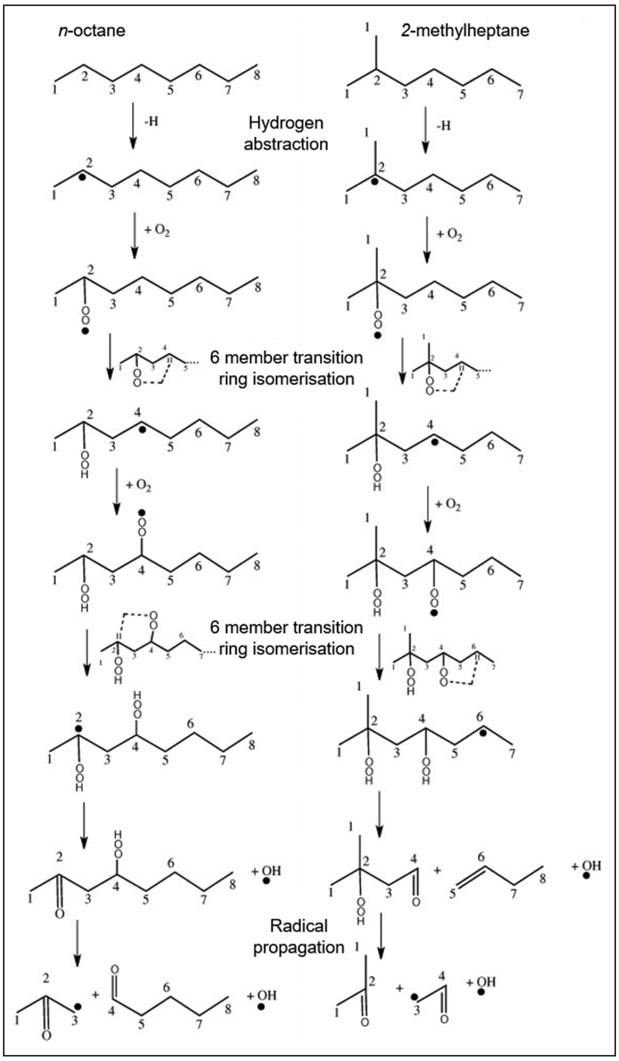

Figure 2. Initial low-temperature branching reactions of (a) *n*-octane and (b) 2-methylpentane.
Source: adapted with permission from Elsevier, 2011.[33]

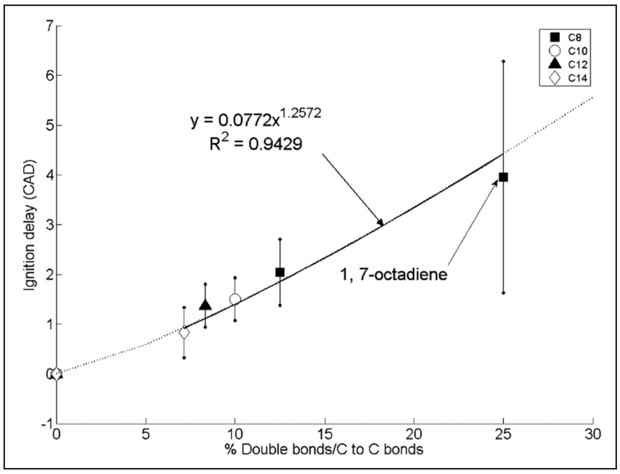

Figure 3. Change in the duration of ignition delay with the percentage of carbon-to-carbon double bonds present in C_8 to C_{14} *n*-alkanes and straight-chain alkenes.
Source: reproduced with permission from SAE International, 2011.[31]
CAD: degrees crank angle.

ignition delay was equivalent to, or more significant, than that observed when comparing the *n*-alkane of equal carbon number to the branched alkane to the *n*-alkane of equal straight alkyl chain length as the *iso*-alkane.[31] In Figure 2(b), it can be seen that, whereas the low-temperature branching reactions of 2-methylpentane initiate with hydrogen abstraction from a tertiary carbon atom (the bond strength of which is weaker than those of secondary and primary carbon to hydrogen bonds), the second isomerisation differs from that in the case of *n*-octane as the carbon atom bonded to the first OOH moiety is not included in the second six-member transition ring formed (Figure 2(a)). This is because there are no further hydrogen atoms available for abstraction from this tertiary carbon atom in the case of 2-methylpentane, and the rate of the second isomerisation is therefore slower than that in an *n*-octane-derived radical as hydrogen abstraction from a secondary carbon atom is required.[33]

Degree of unsaturation and positions of double bonds in an alkyl chain

Figure 3 shows the change in ignition delay with the percentage of double carbon-to-carbon bonds present within the total carbon chain length at a constant injection timing of 7.5° CA before top dead centre and at the same constant engine operating conditions as the results presented in Figure 1.[31] It can be seen in Figure 3 that there is a linear increase in ignition delay with increasing degree of chain unsaturation proportional to the percentage of double bonds present, irrespective of the overall carbon chain length. The presence of double bonds within carbon chains decreases the rates of low-temperature reactions (Figure 2), by reducing both the number of secondary hydrogen atoms available for abstraction and the number of sites at which six-member transition rings can form.[34]

Figure 4 shows the ignition delays of *n*-octane, 1-octene, *trans*-2-octene, *cis*-3-octene and *trans*-3-octene relative to a reference fossil diesel in a direct-injection diesel engine at constant injection timing and constant ignition timing.[44] It can be seen in Figure 4 that, at both injection timings, moving the double-bond position of octene from position 1 to position 2 results in an increase in the duration of ignition delay; however, further movement of the double bond towards the centre of the molecule reduces the ignition delay, in the case of both *cis*-3-octene and *trans*-3-octene. This observation is contrary to studies of shorter-chain alkene isomers in rapid compression machines; Tanaka et al.[45] and Vanhove et al.[46] found that moving the position of the double bond progressively towards the centre of a molecule consistently resulted in an increased duration of ignition delay in heptene and hexene *trans* isomers.

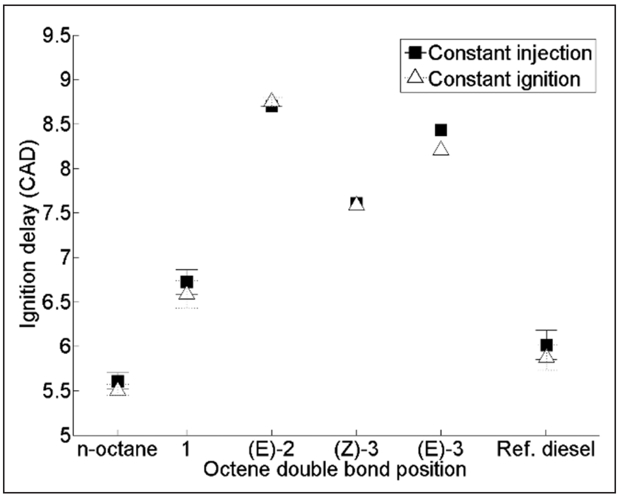

Figure 4. Ignition delay of octene isomers, *n*-octane and reference diesel at constant injection timimg and constant ignition timing.
Source: adapted with permission from Elsevier, 2013.[44]
CAD: degrees crank angle.

Zhang et al.[47] found a similar influence of the double-bond position within the alkyl chain of a fatty acid ester in motored premixed combustion in a Cooperative Fuels Research engine, with the shortest duration of ignition delay exhibited by methyl nonanoate, followed by methyl *trans*-2-nonenoate, and with the longest ignition delay observed in the case of methyl *trans*-3-nonenoate.

Fridlyand et al.[48] investigated the relative reactivities (using speciation of stable intermediates by gas chromatography) of 1-decene, *cis*-2-decene, *cis*-5-decene and *trans*-5-decene in a shock tube at conditions (40–66 bar and 850–1500 K) relevant to compression ignition engines. Contrary to studies of shorter-chain alkene isomers,[44–46] reactivity was found to increase with the movement of the double bond towards the centre of the molecule.[48] In the case of hexene isomers, it has been suggested that the decrease in reactivity with the movement of the double bond can be attributed to the decreasing length of the saturated alkyl chains within the molecule, and the concurrent increasing importance of low-temperature reactions involving the double bond.[46,49] Hellier et al.[44] suggested that the initial increase in the duration of ignition delay (Figure 4) in engine tests of octene isomers can be similarly explained by the decreasing length of the residual saturated alkyl chain but that, in moving the double bond from position 2 to position 3, the longer saturated chain lengths relative to hexane and heptane isomers resulted in a net increase in the low-temperature reactivity. Kinetic modelling undertaken by Fridlyand et al.[48] suggested that decene isomers undergo significantly different reaction pathways dependent on the double-bond position and, in a further study investigating methyl *trans*-2-nonenoate, methyl *trans*-3-nonenoate and the analogous alkenes, 1-octene and *trans*-2-octene, found a dissimilar influence of double-bond movement within the alkyl chain in the FAMEs relative to the alkenes.[50]

Figure 4 also shows a reduced duration of ignition delay of *cis*-3-octene relative to that of *trans*-3-octene, and this was suggested to have been due to the requirement for alkenyl and alkenyl peroxy radicals to be in the *cis* arrangement prior to internal isomerisation across the double bond during low-temperature branching reactions.[44,51] However, in the shock tube study of decene isomers by Fridlyand et al.,[48] no discernible difference between the reactivities of *cis*-5-decene and *trans*-5-decene was detected, further highlighting the varying influence of the double-bond position and arrangement with the overall molecular structure.

Oxygen-bearing functional groups: esters, alcohols, ketones and ethers

Figure 5 shows the effects on the duration of ignition delay of adding oxygen to a molecule of constant carbon number in the case of the carbonyl group[43] and as ether linkages.[52] In Figure 5(a), it can be seen that adding an oxygen atom to 5-nonanone to form butyl valerate increases the duration of ignition delay, as does the addition of a further oxygen atom to form di-*n*-butyl carbonate. Conversely, it can be seen in Figure 5(b) that the addition of oxygen atoms within the alkyl chain as ether linkages results in a decrease in ignition delay. In both cases (Figure 5(a) and (b)), the effects of increasing the molar oxygen content have been attributed to changes in the rates of hydrogen abstraction and internal isomerisation during low-temperature branching reactions (Figure 2). The increased oxygen content of a fatty acid ester relative to a ketone (and of a carbonate ester relative to a fatty acid ester) decreases the rate of initial hydrogen abstraction, because of the increasing electronegativity of the functional group,[25] and also decreases the number of alkyloxy radicals formed as the presence of an oxygen atom attached to the alkyl chain decreases the rates of transition ring reactions.[43,53] However, the presence of oxygen atoms within the alkyl chains of ethers increases the rate of hydrogen abstraction (by reduction in the adjacent C–H bond strength), the rates of isomerisation and also subsequent radical propagation.[52,54–56]

By studying various terpenes potentially produced by genetically modified cyanobacteria, Hellier et al.[57] observed that, of the molecules tested which represented a change to only the functional group of geraniol (a C_{10} alcohol), the equivalent aldehyde, geranial, exhibited the largest decrease in the duration of ignition delay. This is consistent with cetane number measurements of aldehydes relative to equivalent alcohols (octanal and octanol[32]); aldehydes are known to be intermediates in the low-temperature reactions of alcohols,[58] the higher reactivity of which can be attributed to the relative ease with which peroxy radicals may be

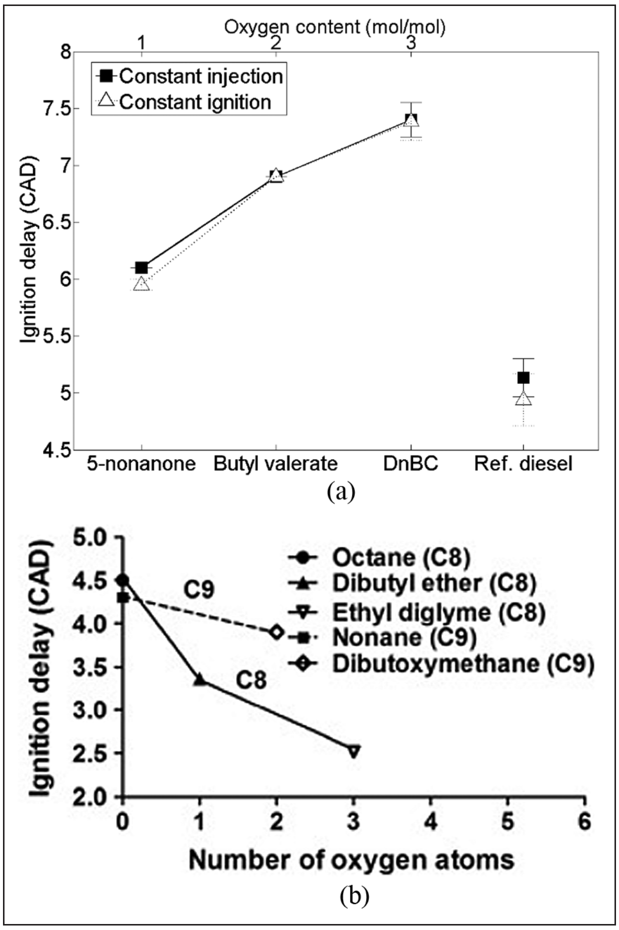

Figure 5. Effect of the molecular oxygen content on ignition delay of (a) di-*n*-butyl carbonate, butyl valerate and 5-nonanone and (b) C_8 and C_9 ethers.
Source: adapted with permission from the American Chemical Society, 2013[43] and reproduced with permission from Elsevier, 2015.[52]
CAD: degrees crank angle; D*n*BC: di-*n*-butyl carbonate.

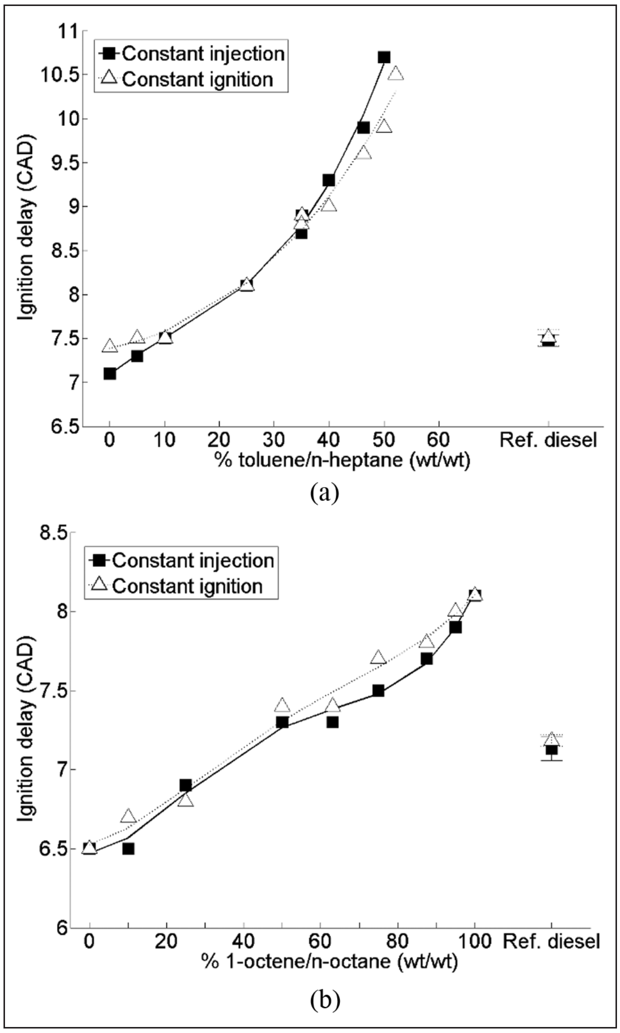

Figure 6. Durations of ignition delay of (a) toluene–*n*-heptane mixtures and (b) 1-octene–*n*-octane mixtures at constant injection timing and constant ignition delay timing.
Source: adapted with permission from The Combustion Institute, 2013.[60]
CAD: degrees crank angle.

formed, requiring the abstraction of a single hydrogen atom without the addition of oxygen.[59]

Many studies have observed an increase in the ignition delay of molecules containing oxygenated functional groups in the terminal position relative to those of alkanes or alkenes of equivalent alkyl chain length.[40,52,53] However, in the study of terpenes by Hellier et al.,[57] where the alkyl moiety present was both branched and unsaturated, the equivalent alkene, citronellene, was of significantly poorer ignition quality than those of the various oxygenated molecules tested.

Binary mixtures including aromatic molecules

Figure 6 shows the duration of ignition delay of binary toluene–*n*-heptane and 1-octene–*n*-octane mixtures relative to a reference fossil diesel at constant injection timing and constant ignition timing. In Figure 6(a), it can be seen that increasing the percentage of toluene present in the toluene–*n*-heptane binary mixtures from 0% to 30% results in a near-linear increase in ignition delay for both timings, and while at toluene levels greater than 35% toluene there continues to be a linear increase in ignition delay, the gradient of this relationship increases significantly.[60] The ignition retarding effect of toluene addition has also been observed in both homogeneous charge compression ignition engines[61] and Cooperative Fuels Research engines,[62] and in the study of alkylbenzenes by Koivisto et al.,[63] where binary toluene–*n*-alkane mixtures were found to have longer durations of ignition delay than the alkylbenzene of corresponding alkyl chain length. Figure 6(b) shows that increasing the percentage of 1-octene present in 1-octene–*n*-octane mixtures also results in a linear increase in the duration of ignition delay; however, in contrast with the toluene–*n*-heptane mixtures, the gradient of this relationship remains almost constant over the whole range of 1-octene additions.[60]

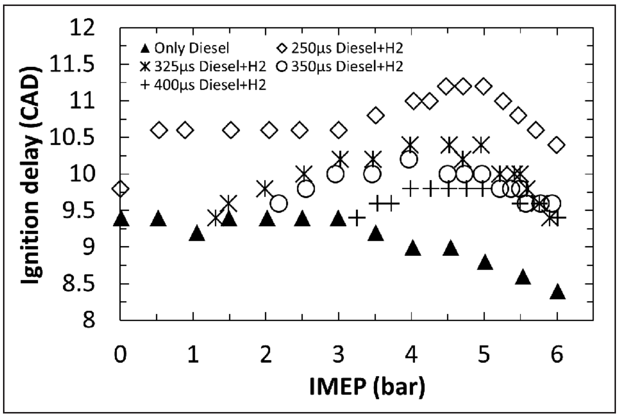

Figure 7. Durations of ignition delay for H_2–diesel co-combustion experiments carried out at a fixed direct-injection diesel fuel flow rate and an increasing level of intake air-aspirated hydrogen addition to increase the engine load.
Source: adapted with permission from Elsevier, 2014.[65]
CAD: degrees crank angle; IMEP: indicated mean effective pressure.

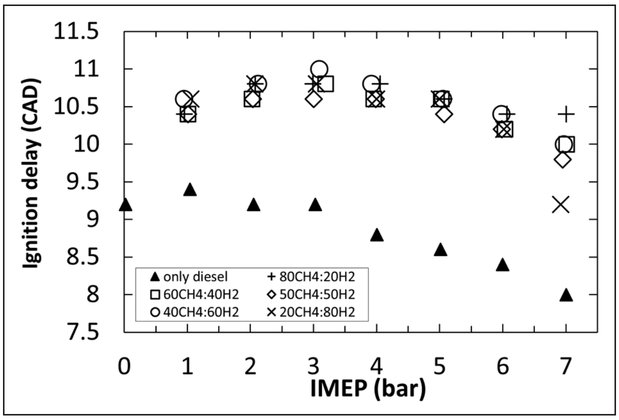

Figure 8. Durations of ignition delay for experiments combusting CH_4–H_2 mixtures pilot ignited by a fixed flow of diesel fuel for different engine loads (IMEPs) and different CH_4–H_2 mixture proportions.
Source: adapted with permission from Elsevier, 2016.[67]
CAD: degrees crank angle; CH4: CH_4 (methane); H2: H_2; IMEP: indicated mean effective pressure.

The non-linear effect of toluene addition on the duration of ignition delay has been suggested to be attributable, in both premixed combustion systems[61,64] and direct-injection compression ignition combustion[60] (Figure 6(a)), to the inhibiting effect of toluene on the low-temperature branching reactions of *n*-alkanes. At low temperatures, toluene can be oxidised via the abstraction of a hydrogen atom from the methyl group by oxygen or preferentially non-selective OH radicals, resulting in benzyl radicals that are thermally stable below 1000 K and cannot be further oxidised.[59,61,64] This consumption of an OH radical into a stable benzyl species therefore slows the rates of *n*-alkane branching reactions, in which the radical would otherwise be available to participate.

Premixed hydrogen–methane pilot-ignited combustion

Figure 7 shows the variation in the duration of ignition delay period for hydrogen–diesel (H_2–diesel) fuel co-combustion tests carried out by Talibi et al.[65] on a naturally aspirated direct-injection diesel engine. Although hydrogen flames are expected to have high propagation rates owing to the fast and thermally neutral branching-chain reactions of hydrogen relative to the slower endothermic low-temperature reactions of larger fuel molecules,[66] hydrogen has an appreciably lower cetane number than that of fossil diesel fuel[66] and cannot be readily ignited by means of compression in modern diesel engines. Therefore, for the experiments presented in Figure 7, the duration of ignition delay is that of the diesel fuel, the combustion of which resulted in ignition and flame propagation through the intake-air-aspirated hydrogen.

Figure 7 shows that for each set of tests, as the engine load is increased (by hydrogen addition, while the diesel fuel flow is kept constant), there is a general trend of increasing ignition delay, which peaks and subsequently decreases with further hydrogen addition. The initial increase was attributed to the displacement of intake oxygen by hydrogen, which led to a decrease in the rates of low-temperature fuel breakdown reactions (Figure 2), thereby delaying autoignition. At higher engine loads (and thus higher levels of hydrogen addition and a subsequently richer hydrogen–air (H_2–air) stoichiometry) it was suggested that the reduction in ignition delay arises from a higher in-cylinder temperature which offsets the reduced oxygen level.[65]

Figure 8 shows similar trends in ignition delay when burning methane–hydrogen (CH_4–H_2) mixtures, pilot ignited by diesel fuel, in a compression ignition engine[67] as seen in the case of hydrogen only intake aspirated mixtures (Figure 7). Furthermore, Figure 8 shows that, for the same engine load, the ignition delay period is considerably longer for all CH_4–H_2 mixtures relative to only diesel fuelling. Whereas diesel fuel is expected to burn at near-stoichiometric conditions,[68] the aspirated CH_4–H_2 mixture is relatively lean and cannot be expected to participate chemically in the diesel fuel low-temperature reactions during the ignition delay period (Figure 2). It was also speculated that the aspirated CH_4–H_2 mixture slows oxidation reactions by diluting the intake oxygen, resulting in an increased ignition delay period.[67]

Influences of the fuel molecular structure on engine exhaust emissions

NO_x

In several studies, a strong relationship has been observed between the duration of fuel ignition delay (which is affected by fuel molecular structure as

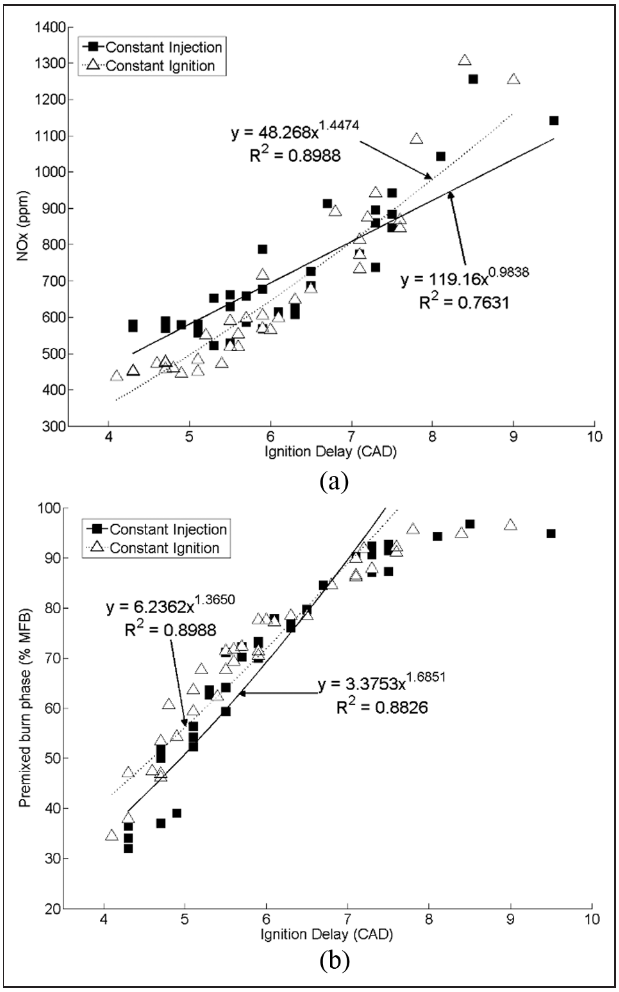

Figure 9. Effect of single-component fuel ignition delay on (a) the exhaust emissions of NO_x and (b) the premixed burn fraction at constant injection timing and constant ignition timing. Source: reproduced with permission from SAE International, 2011.[31]
NOx: nitrogen oxides; CAD: degrees crank angle; MFB: mass fraction burned.

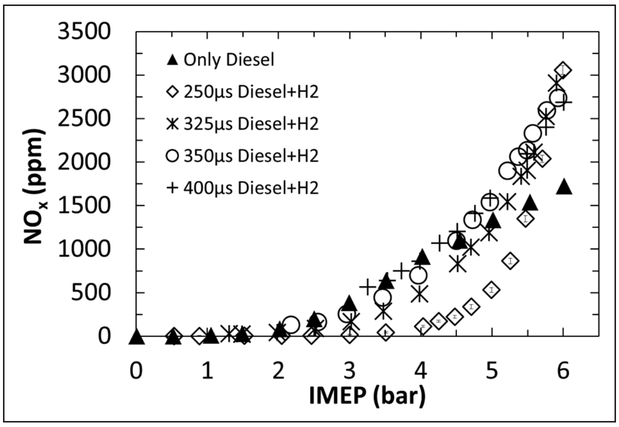

Figure 10. Variation in the exhaust emissions of NO_x at various engine loads and various H_2–diesel fuel proportions. Source: adapted with permission from Elsevier, 2014.[65]
NO_x: nitrogen oxides; H2: H_2; IMEP: indicated mean effective pressure.

discussed in the second section of this paper) and the level of exhaust NO_x emissions.[4,10,31,36,37,69] Figure 9 shows the effect of the variation in ignition delay of *n*-alkanes and 1-alkenes on the exhaust emissions of NO_x and the premixed burn fraction at constant injection timing and constant ignition timing.[31] In Figure 9(a), it can be seen that there is a linear increase in the exhaust level of NO_x emissions whereas, in Figure 9(b), it is apparent that there is a concurrent increase in the extent of the premixed burn fraction with increasing ignition delay. The NO_x emissions during diesel combustion are known to be strongly dependent on the in-cylinder temperature, with the thermal oxidation of nitrogen (also known as the Zeldovich[70] mechanism) dominating formation. Therefore, in Figure 9(a), the increase in NO_x emissions with increasing duration of fuel ignition delay can be attributed to the increased time available for fuel–air mixing prior to the start of combustion, with a resultant increase in the premixed burn fraction (Figure 9(b)) and a higher peak heat release rate, and thus higher in-cylinder temperatures.[31]

In the co-combustion of intake-air-aspirated hydrogen with fossil diesel, some investigators have reported an increase in NO_x emissions, particularly when operating with near-stoichiometric H_2–air mixtures, attributed to the faster burning rates of hydrogen relative to diesel and the resulting higher in-cylinder gas temperatures.[71–73] However, when operating at specific engine load conditions and for advanced diesel fuel injection timings, considerable reductions in exhaust NO_x emissions with H_2–diesel fuel co-combustion have been observed in other studies.[74–76]

Figure 10 shows the concentration of exhaust NO_x emissions for H_2–diesel fuel co-combustion experiments conducted by Talibi et al.,[65] utilising a fixed flow rate of the pilot diesel fuel and with the engine load increased by increasing the hydrogen level. In Figure 10, for a diesel injection duration of 250 µs, levels of NO_x emitted remain at approximately 20 ppm until the increase in hydrogen results in an engine load (IMEP) of 4 bar, beyond which the further addition of hydrogen results in a rapid increase in NO_x emissions. A similar trend was observed in the engine tests conducted by Christodoulou and Megaritis,[77] in which up to 8 vol % of the intake air was replaced by hydrogen. No significant difference in the NO_x emissions was observed at low-engine-load conditions; this was attributed to the smaller thermal boundary layer of the hydrogen flame which enhanced heat rejection and offset the higher adiabatic flame temperature of hydrogen. At higher loads, the NO_x emissions were reported to increase considerably when the proportion of hydrogen energy contribution was increased, which was attributed to the elevated in-cylinder gas temperature.[77] It was suggested by Talibi et al.[65] that, for an IMEP below 4 bar, the relatively lean H_2–air mixture resulted

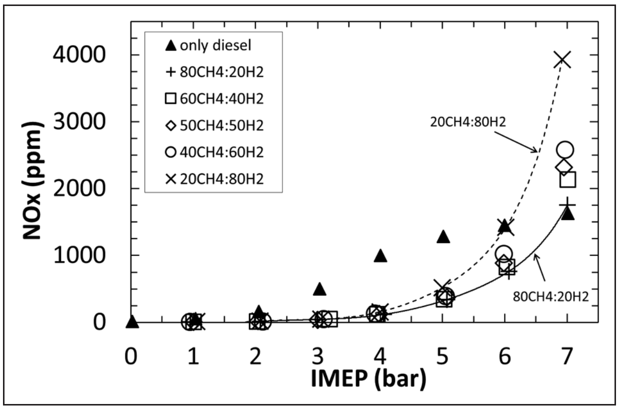

Figure 11. Variation in the exhaust emissions of NO_x at various engine loads and various CH_4–H_2 mixture proportions, at a fixed flow rate of diesel fuel.
Source: adapted with permission from Elsevier, 2016.[67]
NOx: nitrogen oxides; CH4: CH_4 (methane); H2: H_2; IMEP: indicated mean effective pressure.

in a combustion temperature below the threshold for significant NO_x formation. Only at engine loads above 4 bar was the level of hydrogen addition sufficient that the adiabatic flame temperature arising from hydrogen combustion exceeded that required for rapid NO_x formation, resulting in an almost exponential rise in the NO_x emissions (Figure 10). An influence of the adiabatic flame temperature on NO_x emissions in the combustion of fatty acid esters, which is secondary to that of the duration of ignition delay, has been observed where the ignition delays of esters with various degrees of alkyl chain saturation have been equalised by the use of ignition-improving additives.[36,44]

Similar results have been observed when co-combusting CH_4–H_2 mixtures with pilot diesel fuel in compression ignition engines. Increasing the proportion of hydrogen in the aspirated CH_4–H_2 mixture increased heat release rates during the premixed burn fraction and reduced the cycle-to-cycle variability. Furthermore, a considerable increase in emissions of NO_x due to the higher adiabatic flame temperatures of hydrogen relative to methane[78–80] has also been observed. Figure 11 shows the NO_x emissions from a direct-injection diesel engine when combusting CH_4–H_2 mixtures in various proportions and using a constant diesel fuel flow of pilot ignition.[67] As observed in the case of H_2–diesel fuel co-combustion, levels of NO_x emitted remain at a negligible level until the stoichiometry of the aspirated CH_4–H_2 mixture becomes sufficient to reach the threshold temperature (1600–1800 K) which promotes rapid thermal NO_x formation.

Particulate matter

While, when considering the PM emissions from compression ignition engines, an influence of fuel molecular structure via ignition delay is apparent, the relationship is not as direct as in the case of NO_x formation. Observed trends of decreasing exhaust emissions of PM with increasing duration of ignition delay can possibly be attributed to a decreasing diffusion burn fraction (fuel-rich zones which account for the majority of particulate formation[68]) and higher in-cylinder temperatures, which increase the rate of soot oxidation;[31] however, in addition to combustion phasing, the fuel composition can impact on many other parameters important to particulate formation, such as the local stoichiometry and spray characteristics.[81] In order to isolate the direct effects of fuel molecular structure from those of the combustion phasing, many experimental studies on particulate formation have been conducted under carefully controlled conditions such as laboratory flames,[82–86] shock tubes[87–90] and flow reactors.[91–93] Smoke point tests have been widely used as a metric to determine the sooting tendencies of fuels and involve the measurement of the height at which soot is visibly seen to emerge from the tip of a wick-fed diffusion-type flame; a lower smoke point indicates a higher tendency to form soot. There is consensus that in diffusion flames the tendency of hydrocarbon molecules to form soot increases in the following order: *n*-alkanes < isoalkanes < alkenes < cycloalkanes < alkynes < aromatics.

Cyclic and aromatic molecules. In diffusion flame tests of the smoke point, cyclic and aromatic fuels have a far higher propensity to form soot than aliphatic fuels.[82] For example, Velásquez et al.[94] found that a diesel surrogate fuel of *n*-hexane, cyclohexane, benzene and toluene produced five times more soot in a diffusion flame than an *n*-hexane flame. The effects of the side chains of aromatic molecules are complex in that increasing the length of a side chain tends to reduce the sooting tendency, whereas increasing the number of side chains generally leads to an increase in the sooting tendency.[95]

Most studies concerning the effects of fuel aromatic and cyclic compounds on diesel engine combustion have reported an increase in PM emissions with increasing content of either variety of molecule[62,96–99] and, in some instances, a correlation between the engine exhaust emissions and the diffusion flame sooting tendency was observed.[97–99] For example, Bryce et al.[97] and Tsurutani et al.[99] added increasing amounts of aromatic additives to a base fossil diesel fuel in tests undertaken on indirect-injection diesel engines and found that an increase in the aromatic content significantly increased the exhaust emissions of PM, with Tsurutani et al.[99] identifying that the exhaust emissions of PM increased in the following order: monoaromatics < diaromatics < triaromatics. Miyamoto et al.[96] investigated the combustion of a base fuel consisting an *n*-tetradecane and heptamethylnonane with the addition of various monoaromatic and diaromatic compounds. In constant-ignition-delay and constant-overall-equivalence-ratio conditions, the PM emissions increased linearly with increasing carbon-to-hydrogen ratio of the fuel, in both direct-injection and indirect-injection engines. Thus, the addition of diaromatic molecules tended to result in higher PM emissions than the addition of monoaromatic molecules because of the higher carbon-to-hydrogen ratio of the former.

However, some studies on the engine emissions of PM at constant-ignition-delay conditions have reported only a small or a negligible effect of the aromatic content of the fuel.[60,100,101] Xiao et al.[62] investigated binary fuel blends of *n*-heptane with various levels of toluene or methylnaphthalene in an indirect-injection engine, and while the presence of both aromatic compounds resulted in a significant increase in PM emissions, in tests where toluene was gradually replaced with methylnaphthalene (and the ignition delay did not change considerably), no significant difference in the PM emissions was observed. Hellier et al.[60] combusted binary toluene–*n*-heptane mixtures in a compression ignition engine, where the toluene content was varied from 0% to 52% and, although an ignition-improving additive was utilised in order to equalise the duration of the ignition delay and to minimise the effects of combustion-phasing no consistent effect of increasing the toluene content on the PM emissions was observed.

Alkyl chain length and branching. Smoke point tests show that increasing the *n*-alkane chain length increases the propensity of the compound to form soot, as does the addition of branches to an alkyl chain.[82] Similar results have been observed in a flow reactor (at between 850 °C and 1000 °C) and shock tube studies (at near 2000 °C), where isoparaffins and cycloparaffins have been shown to produce higher yields of soot and precursor molecules (benzene and toluene) during pyrolysis.[102] However, when comparing the engine exhaust emissions of two surrogate fuels of low aromatic and sulphur content, Nakakita et al.[103] did not find an increase in PM emissions from the fuel containing 50–70% more branched structures and twice as many cycloalkanes. As the combustion phasing in the case of the engine tests of both fuels was nearly identical, it was concluded that the alkyl chain structure probably had a significant effect on the PM emissions only when the fuels had a very low aromatic content.[103]

Schönborn et al.[36] investigated FAMEs with increasing alkyl chain length of the fatty acid moiety in compression ignition engine tests of single-component fatty acid esters. The engine was operated at three different injection timings (constant injection timing, constant ignition timing and constant duration of ignition delay) and, for all conditions, no discernible impact on PM emissions was found when the alkyl chain length of the FAMEs was varied between 12 carbon atoms and 18 carbon atoms (single component fully saturated FAME fuels of between C_{12}:0 and C_{18}:0). However, a C_{22} ester (C_{22}:0) produced noticeably higher PM mass emissions,

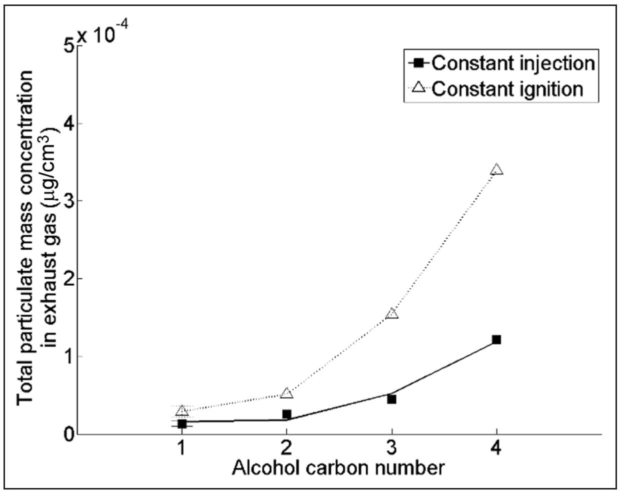

Figure 12. Effect of the straight carbon chain length of the alcohol moiety of the C_{18} fatty acid saturated ester on total particulate mass emissions.
Source: adapted with permission from the American Chemical Society, 2012.[40]

which was attributed to the higher carbon-to-oxygen ratio and higher viscosity of the fuel.

Figure 12 shows the effect of increasing the straight carbon chain length of the alcohol moiety of a saturated fatty acid ester (with a chain length of the fatty acid alkyl moiety of 18 carbon atoms) on the engine exhaust PM emissions.[40] No clear influence of substituting the methyl alcohol moiety of the fatty acid ester with the various longer-chained alcohol moieties on the duration of the fuel ignition delay was observed;[40] however, Figure 12 shows a significant increase in PM emissions with increasing chain length of the alcohol moiety in the fatty acid ester. The increase in the chain length of the alcohol moiety coincided with decreasing molecular oxygen content, increasing viscosity and increasing boiling point;[40] the changes in these properties are all expected to result in increased levels of PM formation and emissions.[81]

Degrees of unsaturation and positions of the double bonds in the alkyl chain. Smoke point tests invariably show that, for molecules with comparable numbers of carbon atoms, the sooting tendency is as follows: alkanes > alkenes > alkynes. For example, Hunt[95] recorded that the fuels *n*-octane, 1-octene, 2-octene and 1-octyne have smoke points that are 149 mm, 99 mm, 99 mm and 24 mm respectively.

The influence of fuel molecule degree of saturation in diesel engine combustion was investigated by Schonbörn et al.,[36] who varied the degree of saturation within the alkyl chain of a FAME of fixed chain length. Increasing the number of double bonds in the alkyl chain resulted in an increase in the particulate mass concentration in the engine exhaust gas, for experiments carried out at constant ignition delay timing and at constant ignition timing. However, in engine tests of binary *n*-octane–1-octene mixtures at constant injection timing and constant ignition timing by Hellier et al.,[60] no clear influence of increasing the proportion of 1-octene was found on the particulate mass concentration measured in the exhaust.

Isotope-labelling techniques have been employed in order to establish whether double-bonded carbon atoms (C = C) tend to contribute to particulate formation to a greater extent than those that contain a single bond. Eveleigh et al.[104] carried out an experimental study where a fatty acid, namely oleic acid (C_{18}:1), was specifically ^{13}C labelled at the double-bonded carbon atoms (oleic acid-9,10-$^{13}C_2$). It was found in tube reactor and diesel engine tests that the labelled double-bonded carbon atoms tended to contribute to PM formation at approximately the same rate as the other carbon atoms in the alkyl chain of oleic acid (Table 1). Similarly, a ^{14}C technique employed by Buccholz et al.[105] showed that the double-bonded carbon atoms in dibutyl maleate contributed to PM formation during diesel engine combustion at the same rate as the average carbon atom in the fuel.

Movement of a single double bond within isomers of octene towards the centre of the alkyl chain was found to result in an increase in PM mass engine exhaust emissions by Hellier et al.[44] at all injection timings, and at constant ignition delay timing *trans*-2-octene was found to produce more nucleation-mode particles (D_p < 50 nm) than 1-octene. This observation is in agreement with the shock tube study of decene isomers by Fridlyand et al.[48] who found an increasing yield of benzene (an important precursor to particulate formation) in the speciation of reaction intermediates by gas chromatography with movement of the decene double bond from position 1 to positions 2 and 5.

Oygen-bearing functional groups. Using the smoke point method, Barrientos et al.[86] investigated the sooting tendencies of a range of C_5 oxygenated compounds. Among the mono-oxygenated compounds tested, the sooting tendencies were determined to be in the following order: aldehydes < alcohols < ketones < ethers. For dioxygenated compounds the order of sooting tendency was as follows: acids < esters < diethers.

In compression ignition engines, oxygenated fuels and fuel additives have been found to reduce exhaust emissions of PM, and the extent of the reduction is mainly dependent on the amount of oxygen present in the fuel. For example, Miyamoto et al.[106] fuelled a direct-injection compression ignition engine with diesel fuel blended with various levels of four oxygenated molecules (di-*n*-butyl ether, ethylhexyl acetate, ethylene glycol mono-*n*-butyl ether and diethylene glycol dimethyl ether). As the overall percentage of oxygen in each fuel blend was increased, a proportional reduction in the particulate mass emissions was observed and, when the oxygen content was about 25–35 % by mass of the fuel, the particulate emissions were reduced to nearly zero. It should be noted that fossil diesel fuel is typically composed of about 20% aromatics, which produce higher levels of soot than alkanes. Therefore, replacing part of the aromatic diesel fuel with a straight-chained hydrocarbon can reduce PM emissions independently of the oxygen content.

Whereas the reduction in the exhaust emissions of PM are mainly correlated with the fraction of oxygen in the fuel, there are known to be differences in the relative effectiveness of different oxygenated molecules in reducing the diesel engine emissions of PM, which have been demonstrated by a number of experimental studies[52,104,106–109] and predicted by numerical kinetic modelling.[110]

Isotope-labelling experiments have been carried out to aid the understanding of how oxygen influences the conversion of carbon to PM. For example, Buchholz et al.[105] found that the carbon atom directly attached to the two oxygen atoms of the ester moiety in dibutyl maleate did not contribute to PM. In further work, Mueller et al.[111] investigated, numerically and experimentally, the combustion of tri(propylene glycol) methyl ester, where oxygen is mainly present as ether linkages, and dibutyl maleate, where oxygen is bound in an ester group (Table 1). They concluded that the distribution of oxygen in tri(propylene glycol) methyl ester is more effective at reducing PM formation than the ester group in dibutyl maleate and that more than 30% of the oxygen in dibutyl maleate is unavailable for soot oxidation.

Eveleigh et al.[112] carried out a similar isotope-labelling experiment and blended a number of alcohols (ethanol, *n*-propanol and isopropanol) and a ketone (acetone) into binary mixtures with *n*-heptane to a level of 10% (molar concentration), which were combusted in a diesel engine and a flow reactor. Similar results were obtained in both systems, where in the case of the alcohols, the carbon atoms bonded to the hydroxyl groups contributed to soot formation in all cases, but to a reduced extent compared with the average carbon atom. In the case of the ketone, the carbonyl carbon atom did not contribute to particulate formation at all, indicating that the bonding and distribution of oxygen influences conversion of a molecule to particulates.

Liquid gaseous fuel co-combustion. Several investigators have reported a reduction in PM emissions during H_2–diesel co-combustion. This has been attributed to a number of factors: the reduction in the overall carbon-to-hydrogen ratio of the combined H_2–diesel fuel mixture, an increased oxidation rate due to a higher in-cylinder gas temperature post ignition, and the formation of OH radicals which potentially enhance oxidation of particulates.[72,74,76,77,113] Figure 13 shows the percentage reduction in the total particulate mass plotted against the percentage reduction in fuel carbon supplied to the engine at constant engine loads for H_2–

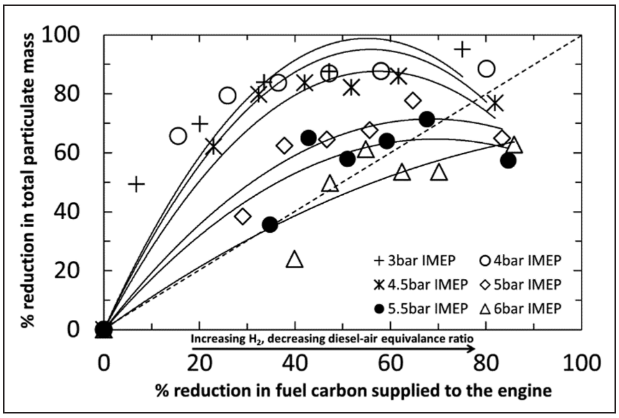

Figure 13. Comparison of the percentage reduction in total particulate mass with percentage reduction in the carbon content of the combustible mixture at constant engine loads for H_2–diesel fuel co-combustion experiments.
Source: adapted with permission from Elsevier, 2014.[65]
IMEP: indicated mean effective pressure.

diesel fuel co-combustion tests.[65] The proportions of diesel fuel and hydrogen were adjusted to achieve constant loads, and the percentage reductions in both particulates and fuel carbon were calculated against the values obtained with the engine operating on only diesel fuel (no hydrogen addition). It can be seen in Figure 13 that, for an engine IMEP below 4 bar, the reduction in PM emissions lies in the top half of the graph, which implies a reduction in the PM emissions beyond that obtained by simple fuel carbon displacement. This suggests that, at engine loads (IMEP) below 4 bar, an increase in the H_2–air stoichiometry (or decrease in the diesel fuel) promotes soot oxidation (or reduces initial soot production), and this offsets any increase in soot formation due to reduced intake oxygen levels. At 6 bar IMEP, the reductions in the PM emissions lie in the bottom half of the graph, suggesting that, although substitution of hydrogen results in a small decrease in particulates, this reduction is considerably lower than expected for the drop in fuel carbon supplied to the engine (Figure 13). Furthermore, at similar high hydrogen substitution levels, several other studies have reported an increase in PM emissions.[72,114] These observations have been attributed to the displacement of significant amounts of intake air (thereby reducing the in-cylinder oxygen concentration), which causes a reduction in rates of fuel oxidation, hence resulting in an increase in PM emissions.[65,72,114]

Conclusions

From compression ignition engine tests on single-component fuels, binary fuel mixtures and pilot-ignited H_2–CH_4 methane combustion, the following conclusions regarding the impacts of fuel molecular structure on diesel engine combustion and emissions characteristics can be made:

1. Increasing the length of a straight alkyl chain decreases the duration of ignition delay by enhancing the rates of hydrogen abstraction and isomerisation during low-temperature reactions. This is apparent in a variety of species that contain alkyl moieties, including *n*-alkanes, alkenes, fatty acid esters and alcohols.
2. Introducing double bonds into an alkyl chain increases the duration of ignition delay by reducing the rates of low-temperature branching reactions. Moving a double bond towards the centre of a fuel molecule can result in both a decrease and an increase in the duration of ignition delay, dependent on the overall alkyl chain length and the presence of oxygenated functional groups.
3. Addition of oxygen atoms to the functional group of a fuel molecule increases the duration of ignition delay. However, the introduction of oxygen atoms within an alkyl chain as ether linkages, or the addition of an oxygenated functional group where the alkyl moiety is of poor ignition quality, can decrease the duration of ignition delay.
4. The presence of aromatic molecules in binary fuel mixtures significantly increases the duration of ignition delay by inhibiting rates of alkyl chain low-temperature reactions. In mixtures of fossil diesel combustion with intake aspirated hydrogen or CH_4–H_2, increasing the levels of the gaseous fuel affect the fossil diesel ignition only by displacement of the intake oxygen.
5. The duration of ignition delay is the primary influence of fuel molecular structure on the exhaust emissions of NO_x. Increased duration of ignition delay results in higher levels of thermal NO_x production via a larger premixed burn fraction and subsequently higher in-cylinder temperatures.
6. The emissions of NO_x from H_2–fossil diesel co-combustion are thermally driven, in that NO_x production from hydrogen combustion commences only at a stoichiometry sufficiently rich for resultant combustion temperatures to exceed those required for significant NO_x formation.
7. When the combustion phasing is held constant, increasing the number of aromatic rings within a hydrocarbon molecule increases PM emissions, as does increasing the alkyl chain length where such changes result in increases in the physical properties (such as the boiling point and the viscosity) which impede fuel–air mixing.
8. Hydrogen promotes PM burnout because of elevated temperatures and higher oxidation rates at low engine loads; however, at higher loads, where the hydrogen addition displaces intake oxygen, PM increases as lower oxygen availability increases particulate formation and reduces rates of PM oxidation.

It can be seen that relatively minor changes to the molecular structure of fuels for compression ignition engines can significantly influence the combustion and emissions characteristics. Therefore, the current and ongoing study of the production routes of alternative fuels is an opportunity to utilise this understanding as to the effects of fuel molecular structure to influence the development of these processes so that the resultant fuels are optimised for clean and efficient operation of compression ignition engines. Furthermore, such understanding can also be exploited for the production of designer fuels for future low-pollutant combustion concepts,[115] e.g. those that require reduced durations of ignition delay or variable control of the ignition timing.[116,117]

Declaration of conflicting interests

The author(s) declared no potential conflicts of interest with respect to the research, authorship, and/or publication of this article.

Funding

The author(s) disclosed receipt of the following financial support for the research, authorship, and/or publication of this article: This work was supported by the UK Engineering and Physical Science Research Council (grant numbers EP/M007960/1 and EP/M009424/1).

References

1. Intergovernmental Panel on Climate Change. Fifth Assessment Report (AR5), IPCC, WMO, Geneva, Switzerland, 2014.
2. European Parliament, Council of the European Union. Directive Regulation (EC) No 715/2007 — type approval of light passenger and commercial vehicles with respect to emissions (Euro 5 and Euro 6) and access to vehicle repair and maintenance information. *Off J Eur Union 2010*.
3. Apsimon H, Amann M, Astrom S and Oxley T. Synergies in addressing air quality and climate change. *Clim Policy* 2009; 9(6): 669–680.
4. Heywood JB. *Internal combustion engine fundamentals*. New York: McGraw-Hill, 1988.
5. Kalghatgi GT. Developments in internal combustion engines and implications for combustion science and future transport fuels. *Proc Combust Inst* 2015; 35(1): 101–115.
6. Zheng M and Reader GT. Energy efficiency analyses of active flow aftertreatment systems for lean burn internal combustion engines. *Energy Conversion Managmt* 2004; 45(15-16): 2473–2493.
7. ASTM D975 - 14a *Standard specification for diesel fuel oils*. West Conshohocken, Pennsylvania: ASTM International, 2008.
8. European Parliament, Council of the European Union. Directive 2009/30/EC of the European Parliament and of the Council of 23 April 2009 amending Directive 98/70/EC as regards the specification of petrol, diesel and gas-oil and introducing a mechanism to monitor and reduce greenhouse gas emissions and amending Council Directive 1999/32/EC as regards the specification of fuel used by inland waterway vessels and repealing Directive 93/12/EEC (Text with EEA relevance). *Off J Eur Union* 2009; L 140: 88–113.
9. European Parliament, Council of the European Union. Directive 2009/28/EC of the European Parliament and of the Council of 23 April 2009 on the promotion of the use of energy from renewable sources and amending and subsequently repealing Directives 2001/77/EC and 2003/30/EC (Text with EEA relevance). *Off J Eur Union* 2009; L 140: 16–62.
10. Graboski MS and McCormick RL. Combustion of fat and vegetable oil derived fuels in diesel engines. *Prog Energy Combust Sci* 1998; 24(2): 125–164.
11. Basha SA, Gopal KR and Jebaraj S. A review on biodiesel production, combustion, emissions and performance. *Renewable Sustainable Energy Rev* 2009; 13(6-7): 1628–1634.
12. Szybist JP, Song J, Alam M and Boehman AL. Biodiesel combustion, emissions and emission control. *Fuel Processing Technol* 2007; 88(7): 679–691.
13. Hoekman SK and Robbins C. Review of the effects of biodiesel on NO_x emissions. *Fuel Processing Technol* 2012; 96: 237–249.
14. Atadashi IM, Aroua MK and Aziz AA. High quality biodiesel and its diesel engine application: a review. *Renewable Sustainable Energy Rev* 2010; 14(7): 1999–2008.
15. Lapuerta M, Armas O and Rodríguez-Fernández J. Effect of biodiesel fuels on diesel engine emissions. *Prog Energy Combust Sci* 2008; 34(2): 198–223.
16. Hoekman SK, Broch A, Robbins C et al. Review of biodiesel composition, properties, and specifications. *Renewable Sustainable Energy Rev* 2012; 16(1): 143–169.
17. Singh SP and Singh D. Biodiesel production through the use of different sources and characterization of oils and their esters as the substitute of diesel: a review. *Renewable Sustainable Energy Rev* 2010; 14(1): 200–216.
18. Hellier P, Purton S and Ladommatos N. Molecular structure of photosynthetic microbial biofuels for improved engine combustion and emissions characteristics. *Frontiers Bioengng Biotechnol* 2015: 20; 3.
19. Akhtar MK, Dandapani H, Thiel K and Jones PR. Microbial production of 1-octanol: a naturally excreted biofuel with diesel-like properties. *Metabolic Engng Commun* 2014;
20. Ghirardi ML. Hydrogen production by photosynthetic green algae. *Indian J Biochem Biophys* 2006; 43: 201–210.
21. Jacob A, Xia A and Murphy JD. A perspective on gaseous biofuel production from micro-algae generated from CO_2 from a coal-fired power plant. *Appl Energy* 2015; 148: 396–402.
22. Anbarasan P, Baer ZC, Sreekumar S et al. Integration of chemical catalysis with extractive fermentation to produce fuels. *Nature* 2012; 491(7423): 235–239.
23. Patel AD, Telalović S, Bitter JH et al. Analysis of sustainability metrics and application to the catalytic production of higher alcohols from ethanol. *Catal Today* 2015; 239: 56–79.
24. Allen JW, Scheer AM, Gao CW et al. A coordinated investigation of the combustion chemistry of diisopropyl ketone, a prototype for biofuels produced by endophytic fungi. *Combust Flame* 2014; 161(3): 711–724.
25. Chuck CJ, Parker HJ, Jenkins RW and Donnelly J. Renewable biofuel additives from the ozonolysis of lignin. *Bioresour Technol* 2013; 143: 549–554.

26. Motte J-C, Sambusiti C, Dumas C and Barakat A. Combination of dry dark fermentation and mechanical pretreatment for lignocellulosic deconstruction: an innovative strategy for biofuels and volatile fatty acids recovery. *Appl Energy* 2015; 147: 67–73.
27. Li S, Li N, Li G et al. Synthesis of diesel range alkanes with 2-methylfuran and mesityl oxide from lignocellulose. *Catal Today* 2014; 234: 91–99.
28. Sargeant LA, Mardell M, Saad-Allah KM et al. Production of lipid from depolymerised lignocellulose using the biocontrol yeast, *Rhodotorula minuta*: the fatty acid profile remains stable irrespective of environmental conditions. *Eur J Lipid Sci Technol* 2016; 118(5): 777–787.
29. Braden DJ, Henao C, Heltzel J et al. Production of liquid hydrocarbon fuels by catalytic conversion of biomass-derived levulinic acid. *Green Chem* 2011; 13(7): 1755.
30. Thamsiriroj T and Murphy JD. A critical review of the applicability of biodiesel and grass biomethane as biofuels to satisfy both biofuel targets and sustainability criteria. *Appl Energy* 2011; 88(4): 1008–1019.
31. Hellier P, Ladommatos N, Allan R et al. The impact of saturated and unsaturated fuel molecules on diesel combustion and exhaust emissions. SAE paper 2011-01-1922, 2012.
32. Yanowitz J, Ratcliff MA, McCormick RL et al. Compendium of experimental cetane numbers. Technical Report NREL/TP-5400-61693, National Renewable Energy Laboratory, Golden, Colorado, USA, 2014.
33. Sarathy SM, Westbrook CK, Mehl M et al. Comprehensive chemical kinetic modeling of the oxidation of 2-methylalkanes from C_7 to C_{20}. *Combust Flame* 2011; 158(12): 2338–2357.
34. Westbrook CK. Chemical kinetics of hydrocarbon ignition in practical combustion systems. *Proc Combust Inst* 2000; 28(2): 1563–1577.
35. Mehl M, Pitz WJ, Westbrook CK et al. Autoignition behavior of unsaturated hydrocarbons in the low and high temperature regions. *Proc Combust Inst* 2011; 33(1): 201–208.
36. Schönborn A, Ladommatos N, Williams J et al. The influence of molecular structure of fatty acid monoalkyl esters on diesel combustion. *Combust Flame* 2009; 156(7): 1396–1412.
37. Koivisto E, Ladommatos N and Gold M. Systematic study of the effect of the hydroxyl functional group in alcohol molecules on compression ignition and exhaust gas emissions. *Fuel* 2015; 153: 650–663.
38. Lapuerta M, Herreros JM, Lyons LL et al. Effect of the alcohol type used in the production of waste cooking oil biodiesel on diesel performance and emissions. *Fuel* 2008; 87(15-16): 3161–3169.
39. Knothe G, Matheaus AC and Ryan TW. Cetane numbers of branched and straight-chain fatty esters determined in an ignition quality tester. *Fuel* 2003; 82(8): 971–975.
40. Hellier P, Ladommatos N, Allan R and Rogerson J. The influence of fatty acid ester alcohol moiety molecular structure on diesel combustion and emissions. *Energy Fuels* 2012; 26(3): 1912–1927.
41. Zhang Y and Boehman AL. Experimental study of the autoignition of $C_8H_{16}O_2$ ethyl and methyl esters in a motored engine. *Combust Flame* 2010; 157(3): 546–555.
42. Schönborn A, Ladommatos N and Bae C. Diffusion- and homogeneous-charge combustion of volatile ethers in a compression ignition engine. *Energy Fuels* 2009; 23(12): 5865–5878.
43. Hellier P, Ladommatos N, Allan R and Rogerson J. Influence of carbonate ester molecular structure on compression ignition combustion and emissions. *Energy Fuels* 2013; 27(9): 5222–5245.
44. Hellier P, Ladommatos N, Allan R et al. The importance of double bond position and *cis–trans* isomerisation in diesel combustion and emissions. *Fuel* 2013; 105: 477–489.
45. Tanaka S, Ayala F, Keck JC and Heywood JB. Two-stage ignition in HCCI combustion and HCCI control by fuels and additives. *Combust Flame* 2003; 132(1-2): 219–239.
46. Vanhove G, Ribaucour M and Minetti R. On the influence of the position of the double bond on the low-temperature chemistry of hexenes. *Proc Combust Inst* 2005; 30(1): 1065–1072.
47. Zhang Y, Yang Y and Boehman AL. Premixed ignition behavior of C_9 fatty acid esters: a motored engine study. *Combust Flame* 2009; 156(6): 1202–1213.
48. Fridlyand A, Goldsborough SS, Brezinsky K et al. Influence of the double bond position on the oxidation of decene isomers at high pressures and temperatures. *Proc Combust Inst* 2015; 35(1): 333–340.
49. Mehl M, Vanhove G, Pitz WJ and Ranzi E. Oxidation and combustion of the n-hexene isomers: a wide range kinetic modeling study. *Combust Flame* 2008; 155(4): 756–772.
50. Fridlyand A, Goldsborough SS and Brezinsky K. Chemical kinetic influences of alkyl chain structure on the high pressure and temperature oxidation of a representative unsaturated biodiesel: methyl nonenoate. *J Phys Chem A* 2015; 119(28): 7559–7577.
51. Bounaceur R, Warth V, Sirjean B et al. Influence of the position of the double bond on the autoignition of linear alkenes at low temperature. *Proc Combust Inst* 2009; 32(1): 387–394.
52. Koivisto E, Ladommatos N and Gold M. The influence of various oxygenated functional groups in carbonyl and ether compounds on compression ignition and exhaust gas emissions. *Fuel* 2015; 159: 697–711.
53. Zhang Y and Boehman AL. Autoignition of binary fuel blends of *n*-heptane and C_7 esters in a motored engine. *Combust Flame* 2012; 159(4): 1619–1630.
54. Cai L, Sudholt A, Lee DJ et al. Chemical kinetic study of a novel lignocellulosic biofuel: di-*n*-butyl ether oxidation in a laminar flow reactor and flames. *Combust Flame* 2014; 161(3): 798–809.
55. Guan L, Tang C, Yang K, Huang Z et al. Experimental and kinetic study on ignition delay times of di-*n*-butyl ether at high temperatures. *Energy Fuels* 2014; 28(8): 5489–5496.
56. Ogura T, Miyoshi A and Koshi M. Rate coefficients of H-atom abstraction from ethers and isomerization of alkoxyalkylperoxy radicals. *Phys Chem Chem Phys* 2007; 9(37): 5133–5142.
57. Hellier P, Al-Haj L, Talibi M et al. Combustion and emissions characterization of terpenes with a view to their biological production in cyanobacteria. *Fuel* 2013; 111: 670–688.
58. Salooja KC. The role of aldehydes in combustion: studies of the combustion characteristics of aldehydes and of

their influence on hydrocarbon combustion processes. *Combust Flame* 1965; 9(4): 373–382.
59. Pilling MJ. *Low-temperature combustion and autoignition*. Amsterdam: Elsevier, 1997.
60. Hellier P, Ladommatos N, Allan R and Rogerson J. Combustion and emissions characteristics of toluene/*n*-heptane and 1-octene/*n*-octane binary mixtures in a direct injection compression ignition engine. *Combust Flame* 2013; 160(10): 2141–2158.
61. Andrae J, Johansson D, Björnbom P et al. Co-oxidation in the auto-ignition of primary reference fuels and *n*-heptane/toluene blends. *Combust Flame* 2005; 140(4): 267–286.
62. Xiao Z, Ladommatos N and Zhao H. The effect of aromatic hydrocarbons and oxygenates on diesel engine emissions. *Proc IMechE Part D: J Automobile Engineering* 2000; 214(3): 307–332.
63. Koivisto E, Ladommatos N and Gold M. Compression ignition and pollutant emissions of large alkylbenzenes. *Fuel* 2016; 172: 200–208.
64. Vanhove G, Petit G and Minetti R. Experimental study of the kinetic interactions in the low-temperature autoignition of hydrocarbon binary mixtures and a surrogate fuel. *Combust Flame* 2006; 145(3): 521–532.
65. Talibi M, Hellier P, Balachandran R and Ladommatos N. Effect of hydrogen-diesel fuel co-combustion on exhaust emissions with verification using an in-cylinder gas sampling technique. *Int J Hydrogen Energy* 2014; 39(27): 15 088–15 102.
66. Karim G. Hydrogen as a spark ignition engine fuel. *Int J Hydrogen Energy* 2003; 28(5): 569–577.
67. Talibi M, Balachandran R and Ladommatos N. Influence of combusting methane-hydrogen mixtures on compression-ignition engine exhaust emissions and in-cylinder gas composition. *Int J Hydrogen Energy* 2017; DOI: 10.1016/j.ijhydene.2016.10.049.
68. Dec JE. A conceptual model of DI diesel combustion based on laser-sheet imaging. SAE paper 970873, 1997.
69. Peirce DM, Alozie NSI, Hatherill DW and Ganippa LC. Premixed burn fraction: its relation to the variation in NO_x emissions between petro- and biodiesel. *Energy Fuels* 2013; 27(7): 3838–3852.
70. Zeldovich YB, Sadavnikov PY and Frank-Kamentskii DA. *Oxidation of nitrogen in combustion*. Moscow: Institute of Chemical Physics, Academy of Sciences of the USSR, 1947.
71. Tsolakis A, Hernandez JJ, Megaritis A and Crampton M. Dual fuel diesel engine operation using H_2. Effect on particulate emissions. *Energy Fuels* 2005; 19(2): 418–425.
72. Varde K and Varde L. Reduction of soot in diesel combustion with hydrogen and different H/C gaseous fuels. In: *5th world hydrogen energy conference*, Toronto, Ontario, Canada, 15–20 July 1984, Vol 4, pp. 1631–1641. Oxford: Pergamon.
73. Naber J. Hydrogen combustion under diesel engine conditions. *Int J Hydrogen Energy* 1998; 23(5): 363–371.
74. Lambe S and Watson H. Optimizing the design of a hydrogen engine with pilot diesel fuel ignition. *Int J Veh Des* 1993; 14(4): 370–389.
75. Tomita E, Kawahara N, Piao Z et al. Hydrogen combustion and exhaust emissions ignited with diesel oil in a dual fuel engine. SAE paper 2001-01-3503, 2001.
76. Saravanan N, Nagarajan G, Sanjay G et al. Combustion analysis on a DI diesel engine with hydrogen in dual fuel mode. *Fuel* 2008; 87(17-18): 3591–3599.
77. Christodoulou F and Megaritis A. Experimental investigation of the effects of separate hydrogen and nitrogen addition on the emissions and combustion of a diesel engine. *Int J Hydrogen Energy* 2013; 38(24): 10 126–10 140.
78. McTaggart-Cowan GP, Rogak SN et al. Combustion in a heavy-duty direct-injection engine using hydrogen-methane blend fuels. *Int J Engine Res* 2009; 10(1): 1–13.
79. Cortés de Zea Bermudez V, Gatts T, Li H et al. An experimental investigation of H_2 emissions of a 2004 heavy-duty diesel engine supplemented with H_2. *Int J Hydrogen Energy* 2010; 35(20): 11 349–11 356.
80. Zhou JH, Cheung CS and Leung CW. Combustion, performance and emissions of a diesel engine with H_2, CH_4 and H_2-CH_4 addition. *Int J Hydrogen Energy* 2014; 39(9): 4611–4621.
81. Tree DR and Svensson KI. Soot processes in compression ignition engines. *Prog Energy Combust Sci* 2007; 33(3): 272–309.
82. Ladommatos N, Rubenstein P and Bennett P. Some effects of molecular structure of single hydrocarbons on sooting tendency. *Fuel* 1996; 75(2): 114–124.
83. Calcote HF and Manos DM. Effect of molecular structure on incipient soot formation. *Combust Flame* 1983; 49(1-3): 289–304.
84. Botero ML, Mosbach S and Kraft M. Sooting tendency and particle size distributions of *n*-heptane/toluene mixtures burned in a wick-fed diffusion flame. *Fuel* 2016; 169: 111–119.
85. Salamanca M, Velásquez M, Mondragón F and Santamaría A. Variations of the soot precursors chemical composition induced by ethanol addition to fuel. *Energy Fuels* 2012; 26(11): 6602–6611.
86. Barrientos EJ, Lapuerta M and Boehman AL. Group additivity in soot formation for the example of C-5 oxygenated hydrocarbon fuels. *Combust Flame* 2013; 160(8): 1484–1498.
87. Alexiou A and Williams A. Soot formation in shock-tube pyrolysis of toluene-*n*-heptane and toluene-iso-octane mixtures. *Fuel* 1995; 74(2): 153–158.
88. Frenklach M, Ramachandra MK and Matula RA. Soot formation in shock-tube oxidation of hydrocarbons. *Symp Combust* 1985; 20(1): 871–878.
89. Frenklach M, Taki S, Durgaprasad MB and Matula RA. Soot formation in shock-tube pyrolysis of acetylene, allene, and 1, 3-butadiene. *Combust Flame* 1983; 54(1): 81–101.
90. Mathieu O, Djebaïli-Chaumeix N, Paillard C-E and Douce F. Experimental study of soot formation from a diesel fuel surrogate in a shock tube. *Combust Flame* 2009; 156(8): 1576–1586.
91. Ruiz MP, Callejas A, Millera A et al. Soot formation from C_2H_2 and C_2H_4 pyrolysis at different temperatures. *J Analyt Appl Pyrolysis* 2007; 79(1-2): 244–251.
92. Esarte C, Abián M, Milleraá et al. Gas and soot products formed in the pyrolysis of acetylene mixed with methanol, ethanol, isopropanol or *n*-butanol. *Energy* 2012; 43(1): 37–46.

93. Esarte C, Milleraá, Bilbao R and Alzueta MU. Gas and soot products formed in the pyrolysis of acetylene-ethanol blends under flow reactor conditions. *Fuel Processing Technol* 2009; 90(4): 496–503.
94. Velásquez M, Mondragón F and Santamaría A. Chemical characterization of soot precursors and soot particles produced in hexane and diesel surrogates using an inverse diffusion flame burner. *Fuel* 2013; 104: 681–690.
95. Hunt RA. Relation of smoke point to molecular structure. *Ind Engng Chem* 1953; 45(3): 602–606.
96. Miyamoto N, Ogawa H, Shibuya M et al. Influence of the molecular structure of hydrocarbon fuels on diesel exhaust emissions. SAE paper 940676, 1994.
97. Bryce D, Ladommatos N, Xiao Z and Zhao H. Investigating the effect of oxygenated and aromatic compounds in fuel by comparing laser soot measurements in laminar diffusion flames with diesel-engine emissions. *J Inst Energy* 1999; 72(493): 150–156.
98. Ladommatos N, Xiao Z and Zhao H. Effects of fuels with a low aromatic content on diesel engine exhaust emissions. *Proc IMechE Part D: J Automobile Engineering* 2000; 214(7): 779–794.
99. Tsurutani K, Takei Y, Fujimoto Y et al. The effects of fuel properties and oxygenates on diesel exhaust emissions. SAE paper 952349, 1995.
100. Ullman TL, Spreen KB and Mason RL. Effects of cetane number, cetane improver, aromatics, and oxygenates on 1994 heavy-duty diesel engine emissions. SAE paper 941020, 1994.
101. Ladommatos N, Rubenstein P, Harrison K et al. The effect of aromatic hydrocarbons on soot formation in laminar diffusion flames and in a diesel engine. *J Inst Energy* 1997; 70(484): 84–94.
102. Takatori Y, Mandokoro Y, Akihama K et al. Effect of hydrocarbon molecular structure on diesel exhaust emissions Part 2: effect of branched and ring structures of paraffins on benzene and soot formation. SAE paper 982495, 1998.
103. Nakakita K, Takasu S, Ban H et al. Effect of hydrocarbon molecular structure on diesel exhaust emissions Part 1: comparison of combustion and exhaust emission characteristics among representative diesel fuels. SAE paper 982494, 1998.
104. Eveleigh A, Ladommatos N, Hellier P and Jourdan A-L. An investigation into the conversion of specific carbon atoms in oleic acid and methyl oleate to particulate matter in a diesel engine and tube reactor. *Fuel* 2015; 153: 604–611.
105. Buchholz BA, Mueller CJ, Upatnieks A et al. Using carbon-14 isotope tracing to investigate molecular structure effects of the oxygenate dibutyl maleate on soot emissions from a DI diesel engine. SAE paper 2004-01-1849, 2004.
106. Miyamoto N, Ogawa H, Nurun NM et al. Smokeless, low NO_x, high thermal efficiency, and low noise diesel combustion with oxygenated agents as main fuel. SAE paper 980506, 1998.
107. Litzinger T, Stoner M, Hess H and Boehman A. Effects of oxygenated blending compounds on emissions from a turbocharged direct injection diesel engine. *Int J Engine Res* 2000; 1(1): 57–70.
108. Stoner M and Litzinger T. Effects of structure and boiling point of oxygenated blending compounds in reducing diesel emissions. SAE paper 1999-01-1475, 1999.
109. Cheng AS, Dibble RW and Buchholz BA. The effect of oxygenates on diesel engine particulate matter. SAE paper 2002-01-1705, 2002.
110. Westbrook C, Pitz W and Curran H. Chemical kinetic modeling study of the effects of oxygenated hydrocarbons on soot emissions from diesel engines. *J Phys* 2006; 110(21): 6912–6922.
111. Mueller C, Pitz W, Pickett L and Martin G. Effects of oxygenates on soot processes in DI diesel engines: experiments and numerical simulations. SAE paper 2003-01-1791, 2003.
112. Eveleigh A, Ladommatos N, Hellier P and Jourdan A-L. Quantification of the fraction of particulate matter derived from a range of ^{13}C-labeled fuels blended into heptane, studied in a diesel engine and tube reactor. *Energy Fuels* 2016; 30(9): 7678–7690.
113. Saravanan N and Nagarajan G. An experimental investigation of hydrogen-enriched air induction in a diesel engine system. *Int J Hydrogen Energy* 2008; 33(6): 1769–1775.
114. Lilik GK, Zhang H, Herreros JM et al. Hydrogen assisted diesel combustion. *Int J Hydrogen Energy* 2010; 35(9): 4382–4398.
115. Lilik GK and Boehman AL. Advanced diesel combustion of a high cetane number fuel with low hydrocarbon and carbon monoxide emissions. *Energy Fuels* 2011; 25(4): 1444–1456.
116. Schönborn A, Hellier P, Aliev AE and Ladommatos N. Ignition control of homogeneous-charge compression ignition (HCCI) combustion through adaptation of the fuel molecular structure by reaction with ozone. *Fuel* 2010; 89(11): 3178–3184.
117. Schönborn A, Hellier P, Ladommatos N et al. 1-hexene autoignition control by prior reaction with ozone. *Fuel Processing Technol* 2016; 145: 90–95.

Appendix 1

Abbreviations

CA	crank angle
CH_4	methane
CO_2	carbon dioxide
FAME	fatty acid methyl ester
GHG	greenhouse gas
IC	internal-combustion
IMEP	indicated mean effective pressure
NO_x	nitrogen oxides
PM	particulate matter
SOC	start of combustion
SOI	start of injection